

A mean-field theory of nearly many-body localized metals

Sarang Gopalakrishnan¹ and Rahul Nandkishore²

¹*Department of Physics, Harvard University, Cambridge, Massachusetts 02138, USA*

²*Princeton Center for Theoretical Science, Princeton University, Princeton, New Jersey 08544, USA*

We consider the properties of a many-body localized system coupled to a generic ergodic bath whose characteristic dynamical timescales are much slower than those of the system. As we discuss, a wide range of experimentally relevant systems fall into this class; we argue that relaxation in these systems is dominated by collective many-particle rearrangements, and compute the associated timescales and spectral broadening. Moreover, if the many-body localization transition is accompanied by a diverging timescale for thermalization, then the self-consistent environment of any region in a nearly localized metal can itself be modeled as a slowly fluctuating bath. Using this observation, we outline a self-consistent mean-field description of the metallic phase near the many-body localization transition. In this nearly localized regime, the spectra of local operators are highly inhomogeneous; the typical local spectral linewidth is narrow, indicating that the relaxation time is much longer than the other dynamical timescales in the system. The local spectral line width is also proportional to the DC conductivity, which is small in the nearly localized regime. This typical linewidth and the DC conductivity go to zero as the localized phase is approached, with a scaling that we calculate.

I. INTRODUCTION

Many-body localized (MBL) states are states of isolated, macroscopic quantum-mechanical systems in which thermal equilibration and transport are absent. MBL states differ from the more familiar “ergodic” states in which a macroscopic system acts as its own bath, thus bringing itself into thermal equilibrium. Since MBL states were first predicted to exist in certain disordered interacting systems^{1–7}, they have been shown to exhibit a number of unusual properties, including orders and phase transitions that are forbidden in equilibrium^{8–10}. The properties of MBL states, such as the absence of intrinsic decoherence and the persistence of topological order in highly excited states, make them potentially valuable resources for quantum computation.

Much of the theoretical work on MBL to date has focused on the deeply localized regime, in which strong-disorder methods can be applied^{9,11} and a simple phenomenological description exists^{12–16}. Such methods do not readily extend to the complementary regime, in which MBL *emerges* from a thermalizing state; indeed, the nature of the MBL-to-ergodic transition in a closed system is at present an unsolved problem.

In Ref. 17 we adopted an alternative approach to studying the emergence of MBL from a thermalizing state: we explored the behavior (specifically, the spectral properties) of an MBL system coupled to a thermalizing bath in the limit of vanishing system-bath coupling. In Ref. 17, we focused on the case of a bath (e.g., a phonon bath) whose frequency bandwidth exceeds the characteristic energy scales of the system. However, there are a number of experimental settings in which the environment of interest has a *narrow* bandwidth (i.e., is slowly fluctuating) compared with the system. For instance, the dominant source of decoherence in low-temperature solid-state systems is the nuclear spin bath, which fluctuates slowly compared with the electronic degrees of freedom.

More generally, slowly fluctuating baths occur intrinsically in systems that are in some sense near an MBL transition: e.g., in disordered dipolar systems^{18–20} or in metals close to a localization transition, energy is transported through a percolating network of widely spaced resonances; the energy scales of this network are much weaker than the nearest-neighbor coupling.

Motivated in part by these observations, the present work discusses relaxation in an MBL system coupled to a bath whose dynamical timescales are much longer than the characteristic timescales of the system. Relaxation in this regime is qualitatively different from that in the wide-bandwidth regime¹⁷: a typical local transition in the system requires much more energy than the bath can supply or absorb; consequently, relaxation takes place through collective rearrangements, which involve increasingly many particles as the bath bandwidth decreases. The associated relaxation timescale goes as a power law of the bandwidth of the bath. We use these results to construct a self-consistent mean-field description of a *nearly localized metal*, viz. a thermalizing system that acts as a slowly fluctuating heat bath for its constituent parts. The nearly localized metal is characterized by local operators having a spectrum that is highly inhomogeneous, fluctuating on a frequency scale Γ which goes to zero as the localized phase is approached. The relaxation timescale is of order $1/\Gamma$. We determine how Γ scales with various parameters, and thus find a self-sustaining mean-field metallic state with an intrinsic relaxation rate that is parametrically slower than the characteristic energy scales of the system. Within our mean-field approximation, this bad metallic state is at least locally stable for arbitrarily weak interactions in the sense that finite sized subregions cannot undergo a transition to the localized phase. However, in a wide parameter range (see Fig. 4), the self-consistent relaxation rate in the bad metal is many orders of magnitude slower than any other relevant timescale, so that the nearly lo-

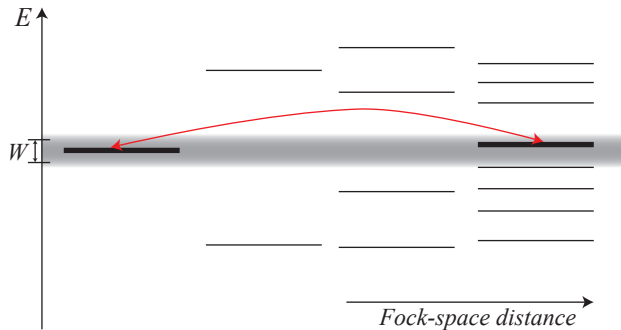


FIG. 1. Schematic illustration of the physics of bandwidth-limited relaxation. Only levels within W of each other can undergo bath-mediated transitions; however, levels that are nearby in energy are typically far apart in real space and/or Fock space.

calized metal cannot be distinguished from true MBL by small-system numerical studies. Such a nearly localized metallic phase should exhibit many of the features of a many-body localized phase coupled to a bath, such as a “soft gap” in the spectra of local operators¹⁷.

Our discussion is arranged as follows. In section II, we discuss the relaxation of an MBL system coupled to a slowly fluctuating “external” bath. In section III we enumerate various experimental instances of MBL systems coupled to slowly fluctuating external baths. In section IV, we turn to the case where the MBL system is coupled to a *self-consistent* (i.e., “internal”) bath with slow dynamics: we first introduce a solvable zero-dimensional model²¹ (see also Ref. 22) that contains the physics of many-particle rearrangements, and then use this model as the basis for a mean-field description of a nearly localized metal²³.

II. SLOWLY FLUCTUATING EXTERNAL BATH

A. Model

We begin by discussing bandwidth-limited relaxation in systems where all many-body eigenstates are localized (the “fully many-body localized” or FMBL regime); such systems have a simple phenomenological description (the “l-bit” model^{12–15}). We assume that our system+bath Hamiltonian is given by $H = H_0 + H_{\text{bath}} + H_{\text{int}}$, where H_0 is the l-bit Hamiltonian for the MBL system¹⁵,

$$H_0 = \sum_i h_i \sigma_i^z + \sum_{ij} J_{ij} \sigma_i^z \sigma_j^z + \sum_{ijk} V_{ijk} \sigma_i^z \sigma_j^z \sigma_k^z + \dots \quad (1)$$

Here, σ_{ij}^z are spin-1/2 degrees of freedom (l-bits) that live on a d -dimensional lattice. The various z - z couplings are short ranged (potentially with exponential tails), and the

many body eigenstates are eigenstates of all the σ_i^z . The σ_i^z are the emergent local conserved quantities, which are related to the physical degrees of freedom by a local unitary transformation of finite depth (equal to the localization length ξ), with potential exponential tails. Flipping a single l-bit typically changes the energy by an amount Δ , the characteristic energy scale of the system.

We now couple the l-bit Hamiltonian to a generic, thermalizing bosonic bath of bandwidth W ; the bosons are taken to live on the links of the original lattice. The system-bath coupling takes the σ^z -conserving form

$$H_{\text{int}} = \gamma \sum_{\langle ij \rangle} (b_{\langle ij \rangle}^\dagger + b_{\langle ij \rangle}) (\sigma_i^+ \sigma_j^- + h.c. + \dots) \quad (2)$$

where the ellipses denote long-range and/or high-order jumps that fall off exponentially with distance, with decay length ξ .

Before turning to the narrow-bandwidth limit, we briefly summarize the results¹⁷ for the wide-bandwidth limit $W \gg \Delta$. In this limit, the factors limiting relaxation are the (weak) system-bath coupling γ (referred to in Ref.17 as g), and the temperature of the bath, T . At low temperatures, $T \ll \Delta$, most spins are frozen in their ground-state configuration; excitations are essentially single-particle in character, and relaxation takes place as in a non-interacting localized state. At high temperatures $T \gg \Delta$, again, the relaxation dynamics shows no signature of many-body processes: the bath is able to place nearest-neighbor l-bit hops on-shell, and these processes therefore dominate relaxation.

These considerations suggest that nontrivial relaxation is likeliest to occur in the parameter regime $W \ll \Delta \ll T$. In the rest of the present section, we shall focus on this regime; we shall further assume that $\gamma \ll W$, so that the bath behaves in an effectively Markovian fashion on the timescales over which the system couples to the bath. Finally, we assume that the bath has a higher heat capacity than the system; for narrow-band baths this entails the assumption that

$$\mathcal{N}(W^2/T^2) \gg 1 \quad (3)$$

where the bath has $\mathcal{N} \gg 1$ times as many degrees of freedom as the system.

B. Relaxation channels

We now discuss three kinds of processes by which a slowly fluctuating bath can induce relaxation in the l-bit model. The general principle is as follows: because $W \ll \Delta/z$ (where z is the coordination number), the bath cannot supply or absorb the energy for a single-l-bit hop. Long-range or high-order processes connect the initial state to many more final states (i.e., have a smaller accessible level spacing), but have a smaller matrix element. For simplicity we shall work with a

bounded bath spectrum having uniform spectral density on the energy interval $[-W/2, W/2]$. The results generalize straightforwardly to cases in which the bath has a Gaussian or other sufficiently sharply peaked spectrum; for a Lorentzian spectrum, however, the dominant processes are typically nearest-neighbor hops that exploit the tails of the Lorentzian (see Appendix). For the bounded bath spectrum, it is clear that the dominant relaxation processes are those for which the effective level spacing is $\sim W$; in what follows, we shall estimate the rates of these processes [Eqs. (4), (5), (6)]. We find that, as $W \rightarrow 0$, relaxation is dominated by multiple-l-bit rearrangements (5). The mechanisms described in this section are analogous to variable-range hopping²⁴, in either real space or Fock space; because we focus on high temperatures and short-range interactions, the physics of the Coulomb gap is not relevant to our analysis.

1. Long-range single l-bit hop

The coupling (2) includes exponentially suppressed long-range hops of the form $\gamma(b + b^\dagger) \exp(-|\mathbf{r}_i - \mathbf{r}_j|/\xi) \sigma_i^+ \sigma_j^-$. To find a single l-bit hop that is on shell to precision W , we must typically hop a distance R , where $\Delta R^{-d} \sim W$. This yields $R \sim (\Delta/W)^{1/d}$, and the matrix element for a hop at this range is $\gamma \exp(-(\Delta/W)^{1/d}/\xi)$. Thus the relaxation rate is

$$\Gamma_a \sim \frac{\gamma^2}{W} \exp(-2(\Delta/W)^{1/d}/\xi). \quad (4)$$

2. Multiple-l-bit rearrangements

In addition to long-range hops, Eq. (2) includes terms of the form $\gamma(b + b^\dagger) \sum \sigma_i^+ \sigma_j^- \sigma_k^+ \dots$ (which are analogous to the many-body rearrangements discussed later in the zero-dimensional case). In order to place the system on shell to within W one must generically rearrange all the l-bits in a volume of linear dimension \hat{n} , where $\Delta \exp(-s(T)\hat{n}^d) \sim W$. Here $s(T)$ is the entropy per l-bit, which interpolates between the limits $s(\infty) = \ln 2$ and $s(0) = 0$, and measures the fraction of spins that are free to flip (see discussion in Ref.17 for details). Because excitations are localized in Fock space as well as real space (see Sec. IV below, as well as Refs. 4 and 21), the corresponding matrix element is $\sim \gamma \exp(-\hat{n}/\xi - \hat{n}^d/\Xi)$, where ξ, Ξ are the real-space and Fock-space localization lengths respectively. In $d > 1$, for small W , this is to leading order

$$\Gamma_b \sim \frac{\gamma^2}{W} \left(\frac{W}{\Delta} \right)^{\frac{1}{\Xi s(T)}} \quad (5)$$

This power-law dependence holds more generally in $d = 1$, but with Ξ replaced by $\xi\Xi/(\xi + \Xi)$.

3. Higher-order coupling to bath

A third channel for relaxation involves going to high order in the system-bath coupling, rearranging all l-bits within a volume of linear dimension $\hat{n} \geq n_c$, where $\Delta \exp(-s(T)n_c^d) \sim n_c^d W$. The approximate solution is when $\hat{n} \sim \left(\frac{1}{s(T)} \log(\Delta/W) \right)^{1/d}$. This gives a relaxation rate (for large \hat{n})

$$\Gamma_c \sim \frac{\gamma^{2\hat{n}^d}}{W \Delta^{2\hat{n}^d - 2}} \sim \frac{\gamma^2}{W} \left(\frac{W}{\Delta} \right)^{\frac{2 \log(\Delta/\gamma)}{s(T)}} \quad (6)$$

where in the first line we have assumed that all the intermediate virtual states are off-shell by the typical amount Δ .

In the limit $\gamma/\Delta, W/\Delta \rightarrow 0$, the leading relaxation rate is Γ_b , given by Eq.(5).

C. Spectral Properties

We now use the estimate (5) of the relaxation rate in the $\gamma, W \rightarrow 0$ limit to discuss the l-bit spectral function (following Ref.¹⁷). Note that the lineshape is Lorentzian at detunings $\delta\omega \ll \Delta$, because the density of final l-bit states within W of $\delta\omega$ is essentially constant. The width of this Lorentzian can be computed precisely as in Ref. 17; we now briefly review this argument, which will be central in what follows. A typical l-bit i flips at a rate Γ_b , but the flipping of nearby l-bits causes the energy of l-bit i to fluctuate. The resulting linewidth, Γ' , can be computed by the following reasoning¹⁷. A typical l-bit at a distance L from i shifts the frequency of i by an amount $\sim U_0 \exp(-L/\xi)$; when $U_0 \exp(-L/\xi) \geq \Gamma'$, l-bit i is sensitive to spin flips at the distance L . The total linewidth Γ' is thus given by adding up the spin-flip rates Γ_b of all l-bits to which i is sensitive; i.e., $\Gamma' = L_c^d \Gamma_b$ where L_c is defined self-consistently by $L_c = \xi \log(U_0/\Gamma')$. Solving for L_c , we find that this linewidth is given by

$$\Gamma' = \Gamma_b s(T) \xi^d \ln^d \left(\frac{U_0}{\Gamma_b s(T) \xi^d} \right), \quad (7)$$

up to $\log(\log)$ corrections, where the entropy factor $s(T)$ simply accounts for the fact that some fraction of the l-bits may be ‘inactive’ at a given bath temperature T . This linewidth can in principle be directly measured by, e.g., a tunneling experiment, or equivalently as the spin-echo decay rate²⁵.

We note in passing that an additional spectral feature is possible if the system-bath coupling has diagonal (i.e., pure dephasing) terms of the form $\sigma^z(b^\dagger + b)$, and if the detuning $\delta\omega < W$. In this special case, the system can put itself ‘on shell’ by borrowing energy from the bath without needing to undergo a collective rearrangement. For concreteness let us assume a tip-to-sample matrix

element t , which is much smaller than any other scale in the problem. Absorption of a quasiparticle then proceeds via an intermediate virtual state with detuning $\delta\omega$, where the matrix element to go to the virtual state is t and the matrix element to leave the virtual state by borrowing energy from the bath is γ . Given that the spectral density in the bath is $1/W$, it follows that tunneling proceeds at a rate $t^2\gamma^2/\delta\omega^2W$, such that the tunneling density of states is $\gamma^2/\delta\omega^2W$, in the special case that $\delta\omega < W$, and diagonal couplings to the bath are allowed.

To summarize, although the dependence of the relaxation rate and linewidth on W are very different in the wide- and narrow-bandwidth limits, the phenomenology *as a function of Γ* is identical to the discussion in Ref.17, and results obtained in Ref.17 can be carried over *mutatis mutandis* to the narrow-band bath case, changing only $\Gamma(g)$ to $\Gamma(W)$ given by Eq. (5). We recall in particular that the DC conductivity σ is related to the local linewidth Γ by $\sigma \sim \Gamma$.

D. Intermediate system-bath coupling

We now comment briefly on how these arguments would be modified in the regime of intermediate system-bath coupling, $W \ll \gamma \ll \Delta$, as is typically the case for hyperfine interactions^{26–30}. In this regime our Golden Rule arguments cannot be used directly because of the importance of the back-action of the system on the bath. Let us consider, for concreteness, a single (“central”) system spin at the origin of coordinates, coupled to a lattice of N bath (e.g., nuclear) spins, with a coupling of the form $\gamma \mathbf{S} \cdot \mathbf{S}_{\text{bath}}(j) \exp(-j)$. The bath spins are taken to have local interactions such that the bandwidth is W . One can see immediately that the bath spins within $\log(\gamma/W)$ of the origin get locked to the central spin; these nearby spins are called the “frozen core” in nuclear magnetic resonance^{29,30}, and should be included in the system rather than the bath. For bath spins that are far away, on the other hand, the effective system-bath coupling is $\gamma_{\text{eff}} \lesssim W \ll \gamma$, allowing us to apply our previous analysis.

III. EXPERIMENTAL RELEVANCE

The most common instance of an ergodic, slowly fluctuating external bath in solid-state systems is a nuclear spin bath. The dynamics of such a bath are due to nuclear spin diffusion, $H_{\text{bath}} \sim \sum_{ij} J_{ij} \mathbf{I}_i \cdot \mathbf{I}_j / |\mathbf{r}_i - \mathbf{r}_j|^3$, where the bandwidth associated with J_{ij} is on the order of 10 kHz^{26–28}, which is orders of magnitude smaller than the typical electronic scales. Under typical experimental conditions²⁸, the nuclear spin bath is effectively at infinite temperature. Thus, realizations of MBL that use the electronic spins of (e.g.) nitrogen-vacancy centers in diamond²⁰ are naturally subject to narrow-band relaxation due to this nuclear spin-bath at low temperatures. (In-

deed, power-law dephasing of the electron spins was predicted on unrelated grounds in Refs.^{26,27}.) We should caution, however, that making quantitative predictions for such systems would require one to address various issues specific to the nuclear case that are beyond the scope of this paper. A more *tunable* kind of narrow-bandwidth bath can be realized by placing the MBL system in a high- Q resonator; in this case, the bandwidth of the bath is set by the linewidth of the resonator mode. Our results are also applicable to the experimentally relevant situation of almost MBL states in systems with long-range interactions, $V(R) \sim 1/R^\alpha$ (e.g., dipoles in three or possibly two dimensions²⁰). In these settings, most of the degrees of freedom are almost localized; however, there is a thermalizing network of long-range resonances at a scale R_0 , which can be regarded as an internal bath whose bandwidth, $\sim 1/R_0^\alpha$, is narrow in the strong-disorder limit. Finally, our results can be applied to almost localized systems coupled to phonons or other Goldstone modes, if all phonons at frequencies $\omega > \omega_c$ are localized, with ω_c suitably small (as in Ref.³¹).

IV. SLOWLY FLUCTUATING “INTERNAL” BATH: THE NEARLY LOCALIZED METAL

The central idea in this section is that while the local spectral function deep in the metallic phase is smooth, the local spectral function in the localized phase is made out of delta functions and contains a hierarchy of gaps¹⁷. Thus as the localization transition is approached the local spectral function in the metal should become increasingly inhomogeneous, and should be composed of increasingly narrow lines. We apply the ideas of the previous section to compute the width of a typical spectral line coupled to a self-consistent bath in a mean-field approximation (similar in spirit to Refs.^{32,33}), and hence obtain a mean-field description of the nearly localized metal.

A. Approach

In previous sections we discussed the behavior of a system coupled to an external bath with slow dynamics. However, any region of an isolated quantum system in the thermalizing regime also behaves as if it were connected to an ‘internal’ heat bath, and close to the localization transition this ‘internal’ heat bath should have asymptotically slow dynamics. In what follows we use this observation to develop a simple mean-field theory of the metallic phase near a many-body localization transition. As we shall discuss below, within our mean-field theory we do not find a stable localized phase. However, we do find mean-field solutions in which the relaxation rates are parametrically smaller than the characteristic energy scales of the system.

We work with a model that is closely related to that of Ref. 4. This model is specified in terms of electrons hop-

ping on a lattice with short range interactions, such that electrons within a correlation length L (in real space) are strongly coupled, but electrons further apart than L (in real space) are weakly coupled. It is important that L be much larger than the lattice scale. The system is now carved up into correlation volumes, each of dimension L , and each correlation volume is treated using a zero-dimensional model of an interacting quantum dot, which we treat in the manner of Ref. 21. The analysis proceeds as follows: in Sec. IV B we compute the relaxation rate of each quantum dot, subject to a slowly fluctuating external bath; in Sec. IV C we specify the nature of the interdot coupling; and in Sec. IV D we replace the external bath from Sec. IV B by a self consistent internal bath, and calculate the relaxation rate due to the interdot coupling. In Sec. IV E we use these results to obtain a self consistent mean field description of the nearly localized metal. While we shall use the terminology of (implicitly quantum-mechanical) “baths” throughout, most of our calculations can be reinterpreted in terms of a quantum dot coupled to an appropriate self-consistent classical noise field^{34, 35}.

B. Quantum dot coupled to slowly fluctuating bath

The first step in constructing our mean-field theory is to estimate the relaxation rate of a level in the zero-dimensional model of Ref. 21 in the presence of a slowly fluctuating (external) bath. We therefore begin by reviewing some results on this model, which consists of a quantum dot with dimensionless conductance $g = E_T/\Delta$, where E_T is the Thouless energy of the dot (i.e., the rate at which electrons diffuse across the dot) and Δ is the single-particle level spacing³⁶. The electronic states on the dot are described by the Hamiltonian^{21, 37}

$$H_{\text{AGKL}} = \sum_{\alpha=1}^N \varepsilon_{\alpha} c_{\alpha}^{\dagger} c_{\alpha} + V_{\alpha\beta\gamma\delta} c_{\alpha}^{\dagger} c_{\beta}^{\dagger} c_{\gamma} c_{\delta} \quad (8)$$

where the statistics of ε_{α} and of $V_{\alpha\beta\gamma\delta}$ are specified, up to an overall interaction strength λ , by random-matrix theory³⁸.

We now briefly review the closed-system behavior of the Hamiltonian (8), focusing on its eigenstates. For $\lambda = 0$, each eigenstate is parameterized by the occupation numbers of N single-particle levels; thus, it forms a vertex of an N -dimensional hypercube (with quenched on-site disorder). The interaction term in H_{AGKL} changes only four occupation numbers at once, and therefore acts as a local hopping term on the hypercube. Ref. 21 argued, by mapping the Fock hypercube onto a Cayley tree with coordination number $K \equiv g^3/6$, that the many-body eigenstates undergo a transition as a function of λ between a low-energy localized regime (in which the eigenstates are localized in Fock space, in the sense that their amplitudes at a point on the Fock hypercube decrease exponentially

with distance from some central site³⁹) and a high-energy delocalized regime (sufficiently deep in this delocalized regime, the eigenstates are “ergodic,” i.e., spread evenly over all configurations with the appropriate energy). The transition point can be approximately estimated by comparing the typical matrix element λ to the accessible level spacing at a given energy $\delta_m(\varepsilon) \simeq \Delta^3/\varepsilon^2$. For sufficiently small λ , all eigenstates on the dot are localized. We shall assume in what follows that we are in this regime, where the isolated quantum dot is fully many body localized. The localization length in Fock space will in general depend on energy. To treat this energy-dependence correctly one would have to go beyond the Cayley-tree model⁴⁰. For simplicity, we ignore the energy dependence of the Fock space localization length, and work with a quantum dot on which all states are localized with a single characteristic Fock-space localization length Ξ .

We now imagine coupling the dot model (8) to a generic, ergodic bath. The bath-mediated interaction is taken to have the particle-number-conserving form

$$H_{\text{int.}} = \gamma \sum_{\alpha, \beta} c_{\alpha}^{\dagger} c_{\beta} (b^{\dagger} + b), \quad (9)$$

where the b 's are the excitations of the bath, which we assume to be bosonic. The bath excitations are taken to have a bounded spectrum in the range $[E - W/2, E + W/2]$, where in general $E \neq 0$.

We now compute the relaxation rate of an excited particle due to hopping, to leading order in small γ/W . At $W = 0$, a system prepared at a particular vertex of the Fock hypercube remains localized near that vertex. At non-zero W , the system can relax by hopping to vertices with a different value of the system energy ε , by borrowing the missing energy from the bath. However, the bath can only supply or absorb energies that are within a range W of E , while neighboring vertices on the Fock hypercube have a level spacing $\delta_m \gg W$, so that nearest-neighbor hops are not, in general, on shell to within W . To find a vertex that differs in energy by less than W , a particle must tunnel to the \hat{n} th neighbor, where $\delta_m K^{-\hat{n}} \leq W$ i.e. $\hat{n} \geq n_c = \log(\delta_m/W)/\log K$. However, the matrix element for a long range hop is of order $\exp(-\hat{n}/\Xi)$, because of the exponential localization of states on the Fock hypercube. Summing over all distances $n \geq n_c$ in a saddle point approximation, we find that the Golden-rule estimate of the relaxation rate Γ is

$$\Gamma(W) = \frac{\gamma^2}{W} \left(\frac{W}{\delta_m} \right)^{2/(\Xi \log K)} \quad (10)$$

This defines a timescale for relaxation $t_{\text{relax}} \sim \gamma^{-2} W^{1 - \frac{2}{\Xi \log K}}$, so the relaxation time diverges as $W \rightarrow 0$. Physically, this divergence of \hat{n} and the consequent slow relaxation arise because finding a transition which is on shell to precision W requires increasingly large rearrangements of the system. Once W [Eq. (10)] becomes smaller

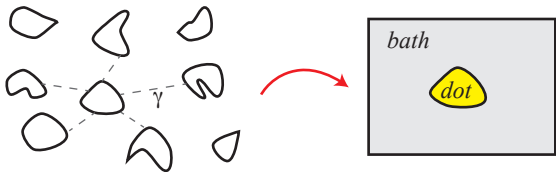


FIG. 2. Schematic description of our mean-field approach. We consider a lattice of statistically similar multilevel quantum dots, and approximate this as a single quantum dot coupled to a slowly fluctuating bath.

than the total many body level spacing of the dot (which is exponentially small in N), then the dot reverts to being fully localized despite the coupling to the bath, since we can no longer find transitions that are on shell to a precision W .

We note that the discussion above applies for a Lorentzian bath only when $\Xi \log K > 1$; otherwise (see Appendix) relaxation is dominated by lowest-order processes that exploit the tails of the Lorentzian. The two cases $\Xi \log K > 1$ and $\Xi \log K \leq 1$ are both taken into account in what follows.

C. Setup of the coupled-dot problem

We now make use of the insight that the AGKL quantum dot model²¹ can be regarded as an effective description for a region with linear dimension of order the correlation length L , which sees a bath due to the other quantum dots to which it couples through the interaction (Fig. 2)⁴¹. It is important for our purposes that the Fock space for each quantum dot be large, i.e., that L be large, for reasons that will become apparent shortly. A similar setup was employed in⁴ when establishing stability of the MBL phase; however, we are not aware of any work that uses such an approach to describe the regime near the MBL transition.

Following Ref.⁴, then, we consider an array of statistically similar quantum dots coupled through a number-conserving interaction of the form $\gamma/\sqrt{zN^2} \sum_{IJ} \sum_{\alpha\beta\gamma\delta} \mathcal{K}_{IJ} c_\alpha^\dagger(I) c_\beta(I) c_\gamma^\dagger(J) c_\delta(J)$, where I and J label different quantum dots, z is the coordination number of the array, N is (as before) the number of single-particle levels on each quantum dot, and the coupling \mathcal{K}_{IJ} decays exponentially with distance between dots, with a decay length of order the size of the dots. We now assume a mean-field decoupling in which dot I is self-consistently coupled to an environment consisting of all the other dots: i.e., $\gamma/\sqrt{zN^2} \sum_{IJ} \mathcal{K}_{IJ} c_\alpha^\dagger(I) c_\beta(I) c_\gamma^\dagger(J) c_\delta(J) \sim \gamma/\sqrt{zN^2} \sum_{I\alpha\beta} c_\alpha^\dagger(I) c_\beta(I) m(I)$, where $m(I) = \sum_{J\gamma\delta} \mathcal{K}_{IJ} c_\gamma^\dagger(J) c_\delta(J)$.

We now ask whether states on the dot can relax by

‘borrowing’ energy from the environment. The environment consists of all allowed transitions in the other quantum dots. If the other quantum dots are localized, then the spectral function of the environment is made up of delta functions. In this case we will not be able to find a transition in the environment that places the transition in the dot exactly on shell. As a result, a localized quantum dot placed in a localized environment will remain localized. In contrast, if the spectral lines in the environment are slightly broadened with a linewidth Γ , then the dot will be able to relax, provided it can find a state, on shell to a precision Γ , to which it can decay. Our objective is to obtain a self consistent mean field theory that describes how this linewidth Γ goes to zero as we approach the localized regime.

An important quantity for our analysis is the spectral function of the self consistent environment. The maximum amplitude in the spectral function of the environment will be wherever there is a spectral line corresponding to single particle transitions on a neighboring dot. The spacing between these peaks is δ_2/z , where $\delta_2 \equiv \Delta^2/\varepsilon$ and $1/\delta_2$ is the accessible two-particle DOS on a single quantum dot. In order for our discussion to make sense, we require that these dominant spectral lines do not overlap. This then requires that $\gamma \ll \delta_2/z$, for reasons that will shortly become clear. We assume the interactions are sufficiently weak that we are operating in this regime.

In addition to the large but sparse features coming from single particle transitions on the neighboring dots, there will be additional features coming from multi-particle transitions. These ‘satellite’ peaks will be much denser than the large peaks coming from single particle transitions on neighboring dots, but they will have an amplitude that is much smaller. The amplitude for peaks coming from multi particle transitions will fall off exponentially with the order of the transition (with decay constant Ξ). The spectral function of the bath will

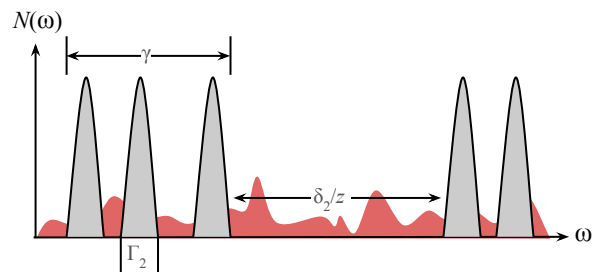


FIG. 3. Spectrum of the self-consistent bath, averaged over a time $1/\Gamma_1$. Due to spectral diffusion, this bath consists of clumps of Γ_2/Γ_1 Lorentzians, each of linewidth Γ_2 , spaced within an interval $\gamma \gg \Gamma_2$ (see main text, section IVD). These clumps of Lorentzians are separated from one another by a spacing $\delta_2 \gg \gamma$. The satellite peaks contribute a broad weak background, indicated in pink.

also have satellite peaks coming from distant dots; however, the amplitude of these satellite peaks falls off exponentially with distance, whereas their density grows only as a power law of distance, so for weak coupling we may ignore the satellite peaks coming from transitions on distant dots. (The Hartree shifts from distant dots will however have to be taken into account, as we will discuss).

D. Self-consistency equations

We shall now derive self-consistent mean-field equations for the model specified in the previous section. These are most naturally expressed in terms of two related but distinct physical quantities, the rate of a typical transition (denoted Γ_1) and the linewidth of a typical transition (denoted Γ_2). Physically, these quantities are related as follows: each transition causes the energy levels on nearby dots to fluctuate via interdot (“Hartree” or diagonal) interactions, contributing to the linewidth; meanwhile, the energy fluctuations of each line (governed by Γ_2) drive real transitions on nearby dots. One can arrive at a naive mean-field theory by ignoring the Hartree interactions and taking $\Gamma_2 \simeq \Gamma_1$; as we shall see below, this would reproduce the results of Refs. 3, 4, and 42. A central result of our paper is that including the Hartree interactions parametrically enhances the stability of the bad metal.

We start by computing the linewidth Γ_2 given the relaxation rate Γ_1 ; the logic here is parallel to that of Sec. II C and Ref. 17. Whenever *any* level undergoes a real transition, it causes the energies of nearby levels to fluctuate, and thus broadens them. Let the decay rate of a typical level on the quantum dot be Γ_1 ; then, following the arguments of Sec. II C and Ref. 17, the full linewidth of this level is given by

$$\Gamma_2 \simeq n_c^d(N^2)\Gamma_1 = \gamma \exp(-n_c) \Rightarrow n_c \approx \log\left(\frac{\gamma}{N^2\Gamma_1}\right) \quad (11)$$

as there are N^2 possible transitions on every dot. (By contrast, in a noninteracting system, $\Gamma_2 = \Gamma_1$.) This then implies that the linewidth Γ_2 is related to the single level decay rate Γ_1 (up to $\log(\log)$ corrections, which we shall neglect) by the relation

$$\Gamma_2 \simeq N^2\Gamma_1 \log^d[\gamma/(N^2\Gamma_1)] \quad (12)$$

In order to arrive at a self-consistent theory, we must supplement Eq. (12) by computing the single-level decay rate Γ_1 given the “bath” linewidth Γ_2 . In the main text we shall assume that $\Gamma_{1,2}$ are spatially uniform. However, our approach can be extended to spatially inhomogeneous systems, as discussed in Appendix B; thus, it can be applied to the case of a system coupled to a boundary bath, and then used to estimate how the decay rates in the system decrease as one moves away from the boundary.

Before we adapt our previous results to the case of a self-consistent bath, we must first address a couple of subtleties. The first subtlety involves the applicability of the Golden Rule. In the regime of interest, the self-consistent linewidth Γ_2 must be smaller than the matrix element $\gamma/\sqrt{zN^2}$. Thus, it is not *prima facie* appropriate to use the Golden Rule to estimate decay rates, and, indeed, a simple application of the Golden Rule using the *averaged* bath spectrum gives evidently incorrect results²¹. However, as we now argue, one can still self-consistently apply the Golden Rule if one works with *typical* bath spectra³³, by the following reasoning. As we shall see, the fastest decay processes are either lowest-order or very-high-order rearrangements, depending on Ξ . We address these cases separately.

(1) In the regime where lowest-order rearrangements are dominant, these processes always exploit the tails of the bath Lorentzians, which have an approximately constant density of states $\sim \Gamma_2/\delta_m^2$ (i.e., we disregard the possibility of a bath transition being resonant with a system transition, as such nearest-neighbor resonances are rare in the regime of interest). This “Lorentzian-tail” bath is effectively a broad-bandwidth bath with a small density of states $\sim \Gamma_2/\delta_m^2$; this bath is, moreover, thermodynamically large whenever we are self-consistently in the metallic phase. Therefore, we can straightforwardly apply the Golden Rule to compute transition rates, as in Ref. 17.

(2) In the regime where the dominant processes are high-order, the system-bath coupling generically has two kinds of terms: (i) diagonal terms (either Hartree-type shifts $\sim \gamma$ or level-repulsion shifts $\sim \gamma^2/\delta$) that do not themselves change the state of the system *or* the statistics of levels (unlike those in Sec. II D); (ii) off-diagonal terms or real transitions. The matrix element associated with *real* transitions is given (Sec. II) by $\gamma \exp(-\hat{n}/\Xi)$, where $\hat{n} \gg 1$ in the nearly localized metal; as we shall see, this effective matrix element does indeed remain smaller than the self-consistent linewidth as one approaches the transition. On the other hand, processes with larger matrix elements are off-shell and hence of type (i). When averaged over a thermal state, type (i) processes cause the levels on a dot to have a distribution of energies broadened by $\sim \gamma$. This line-broadening is *not* relevant for our purposes, as it occurs even deep in the MBL phase¹⁷, where the system clearly does not act as its own bath. Instead, we are interested in the broadening due to *real* transitions.

The second subtlety involves the appropriate procedure for “averaging” over the positions of bath lines. While the instantaneous spectrum of the bath is made up of spectral lines with linewidth Γ_2 , we are interested in the spectrum averaged over a timescale $\tau \sim 1/\Gamma_1$, the typical timescale on which a single state decays⁴³. A particular level in the environment fluctuates within a range $\sim \gamma$ at a rate Γ_2 . When averaged over timescales $\tau \gg \gamma/\Gamma_2^2$, the level samples the entire range γ and thus has a linewidth $\gamma \gg \Gamma_2$. By contrast, when averaged over

a timescale $1/\Gamma_2 \ll \tau \ll \gamma/\Gamma_2^2$, the center of the level occupies $(\tau\Gamma_2)$ points in this interval, and the effective linewidth is $\tau\Gamma_2^2$ (Fig. 3). Taking $\tau = 1/\Gamma_1$, we find that, assuming $\tau \ll \gamma/\Gamma_2^2$ (an assumption we will check below), the environment has an apparent linewidth $\Gamma_2^2/\Gamma_1 \ll \gamma$.

We are now equipped to compute Γ_1 in the presence of this environment. The decay rate of a single level coupled to this self-consistent environment is then given (using the Golden rule) by

$$\Gamma_1 = \gamma^2 \sum_{n,p} \frac{(\Gamma_2^2/\Gamma_1)}{(\delta E)_{p,n}^2 + (\Gamma_2^2/\Gamma_1)} \exp(-2(n+p)/\Xi) \quad (13)$$

where we sum over all processes that involve an n particle rearrangement in the system and a p particle rearrangement in the bath, assuming that the linewidth is the same for all spectral lines, and where $\delta E_{n,p}$ is the detuning

from the nearest spectral line at that order. In addition, Γ_2 is the self-consistent linewidth, which is distinct from the decay rate Γ_1 as discussed in Sec. II C. We assume that $\delta E_{n,p}$ is of order the spacing between the relevant spectral lines, i.e. $\delta E \approx \delta_m \exp(-(n+p) \log K)$, where we are working at infinite temperature. In the above expression we have assumed that the dominant contribution to the decay rate comes from processes at leading order in γ . This approximation is valid when $\ln(\delta_m/\gamma) \gg 1/\Xi$, so that it is less costly to go to high order in the system or in the bath than to go to high order in the system-bath coupling.

The equation (13) can be rewritten explicitly as

$$\Gamma_1 = \frac{\gamma^2}{(\Gamma_2^2/\Gamma_1)} \sum_{n,m} \frac{\exp(-(n+m)/\Xi)}{1 + (\delta_m \Gamma_1/\Gamma_2^2)^2 \exp(-2(m+n) \log K)}. \quad (14)$$

A little algebra allows us to rewrite (14) as

$$\Gamma_1 = \frac{\gamma^2 \Gamma_2^2}{\delta_m^2 \Gamma_1} \sum_{m,n=1}^{m+n < N_c} \exp \left[-(m+n) \left(\frac{2}{\Xi} - 2 \log K \right) \right] + \frac{\gamma^2 \Gamma_1}{\Gamma_2^2} \sum_{m+n \geq N_c} \exp \left[-(m+n) \frac{2}{\Xi} \right]; \quad N_c = \frac{\log(\delta_m \Gamma_1/\Gamma_2^2)}{\log K} \quad (15)$$

One can straightforwardly see that there are two regimes. For $\Xi \log K > 1$, relaxation is dominated by collective rearrangements and is given by the expression

$$\Gamma_1 \simeq \frac{\gamma^2}{\Gamma_2^2/\Gamma_1} \left(\frac{\Gamma_2^2/\Gamma_1}{\delta_m} \right)^{2/\Xi \log K} \quad (16)$$

whereas for $\Xi \log K < 1$, it is dominated by lowest-order processes that exploit the tail of the Lorentzian, and is given by

$$\Gamma_1 \simeq \frac{\Gamma_2^2}{\Gamma_1} \left(\frac{\gamma}{\delta_m} \right)^2. \quad (17)$$

E. Self-consistent solutions

To understand the nature of our mean-field solutions, it is helpful to first simplify the equations by ignoring the logarithmic factor in Eq. (12). This is qualitatively similar to neglecting the Hartree terms altogether. Making this approximation, we find that, for $\gamma \ll \delta_m$, the stable mean-field solutions are

$$\Gamma_2^{approx.} \simeq \begin{cases} \gamma (\gamma z N^2 / \delta_m)^{\frac{1}{\Xi \log K - 1}} & \Xi \log K > 1, \\ 0 & \Xi \log K \leq 1. \end{cases} \quad (18)$$

(Of course, $\Gamma_1 = \Gamma_2 = 0$ is a solution for all Ξ .) In this approximation, the localization transition occurs precisely at $\Xi \log K = 1$, and has the same scaling as in Refs. 3 and 42; for smaller Ξ , there is no metallic phase until γ is comparable in magnitude to δ_m . Eq. (18) does *not* depend on our choice of a Lorentzian bath; the same result can easily be shown to obtain for a bath with a bounded spectrum. Physically, the point $\Xi \log K = 1$ marks the transition on a Cayley tree³⁹ between a truly localized phase, with finite inverse participation ratio, and an intermediate phase, in which the exponential falloff of the wavefunction amplitude is slower than the exponential growth of sites on the Cayley tree, so that the inverse participation ratio vanishes. In this regime, each site on the Cayley tree has resonant partners at a typical distance $\tilde{N}_c \sim \Xi \log(1/\lambda)/(\Xi \log K - 1)$ [recall that λ is the dimensionless interaction strength on the quantum dot]; consequently, there are branches of the Cayley tree along which the wavefunction does not decay at all. Note that the bandwidth of this resonant network (and hence the inverse lifetime of an individual site⁴²) vanishes with $\Xi \log K$ in the same way as Eq. (18); which process is dominant depends on microscopic details.

The logarithmic correction in Eq. (12) changes this behavior qualitatively. Including this correction, we find the general mean-field solutions are $\Gamma_1 = \Gamma_2 = 0$ and:

$$\Gamma_2^{mf} \simeq \begin{cases} \gamma \left[\frac{(N^2 \gamma / \delta_m)^{1/d}}{(\Xi \log K - 1)/d} W \left(\frac{\{(\Xi \log K - 1)/d\} (1/N)^{(\Xi \log K - 1)/d}}{(N^2 \gamma / \delta_m)^{1/d}} \right) \right]^{d/(\Xi \log K - 1)} & \Xi \log K > 1, \\ \frac{\gamma}{N^2} \exp \left[- \left(\frac{\delta_m}{\gamma N^2} \right)^{1/d} \exp \left(\frac{2}{\Xi d} (1 - \Xi \log K) \right) \right] & \Xi \log K \leq 1. \end{cases} \quad (19)$$

where $W(x)$ is the Lambert function. There is still a wide parameter regime for $\Xi \log K > 1$ in which the naive solution (18) applies, but the scaling changes in the immediate vicinity of $\Xi \log K = 1$ (Fig. 4). The solutions in the two regimes coincide at the “critical” value $\Xi \log K = 1$, at which the decay rate is

$$\Gamma_2^{mf} \simeq \frac{\gamma}{N^2} \exp \left[- \left(\frac{\delta_m}{\gamma N^2} \right)^{1/d} \right] \quad (20)$$

At the level of this analysis, there is a cusp at $\Xi \log K = 1$ [Fig. 4]; we expect that this is an artifact of the saddle-point approximation in which we have computed the decay rate. Starting from large Ξ , the optimal decay channel moves to higher and higher order in perturbation theory (Fig. 6) as Ξ is lowered until very close to $\Xi \log K = 1$, at which it rapidly decreases to lowest-order processes; there is a small window around $\Xi \log K = 1$ at which all orders are equally important, and we do not expect to capture this in a saddle-point calculation. We emphasize however that within our mean field theory, we find a ‘metallic’ solution even for $\Xi \log K \ll 1$, when the single quantum dot calculation as well as the naive calculation that neglects Hartree shifts (18) would find only an insulator. This is an extremely weakly metallic phase, as evidenced by the smallness of the linewidth (stretched exponentially small in γ and double exponentially small in Ξ), and by the inhomogeneity of the local spectrum.

An iterative stability analysis suggests that, within the regime of validity of our theory, this bad metal phase is always stable: for arbitrarily small decay rates, the linewidth of a local level picks up contributions from arbitrarily distant dots, and this prevents it from vanishing (see Appendix B). Thus, while our mean-field theory can access relaxation in a nearly localized metal, it does not capture the localization transition. This does *not* contradict the now well-established fact that the MBL phase exists and is stable in one-dimensional spin chains⁴⁴; for one thing, mean-field theory is typically an unreliable guide to the behavior of one-dimensional systems; for another, even on its own terms our argument does not preclude an MBL phase, but merely suggests that it must exist outside the regime of validity of the mean-field theory.

To elaborate on this second point, we now check the consistency of various assumptions we made in the preceding argument. First, the applicability of the Golden Rule requires that

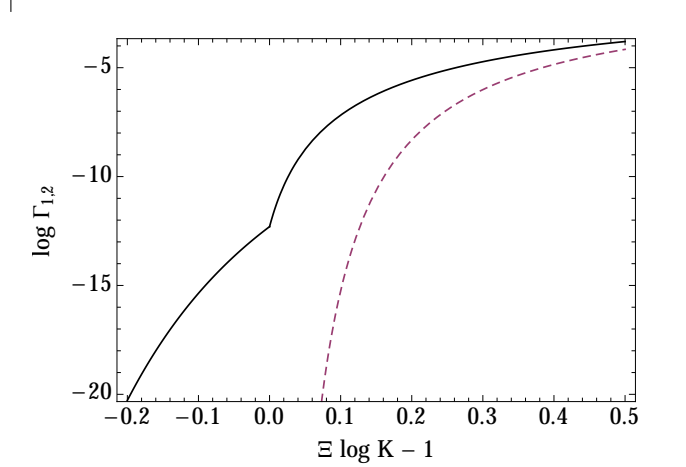


FIG. 4. Solid line: logarithm of the mean-field linewidth Γ_2 as a function of the parameter $\Xi \log K$ ($d = 1$ and $\gamma/N^2 \delta_m = 0.1$). The dashed line shows the linewidth calculated without the log correction; this is parametrically smaller as $\Xi \log K \rightarrow 1$.

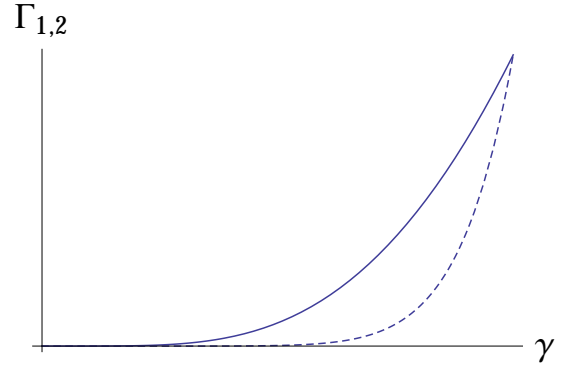


FIG. 5. Solutions $\Gamma_{1,2}$ to the self-consistency equations in $d = 3$ with the logarithmic correction (solid line) and without (dashed line), for $\Xi \log K = 1.1$. The two curves have been rescaled to fit on the same axes.

$$\gamma \{ \Gamma_2^2 / (\Gamma_1 \delta_m) \}^{\min(1, 1/\Xi \log K)} \ll \Gamma_2^2 / \Gamma_1, \quad (21)$$

and second, we assumed that $\gamma \Gamma_1 \gg \Gamma_2^2$, such that the spectral function of the environment is highly inhomogeneous. These assumptions can be combined into the statement that

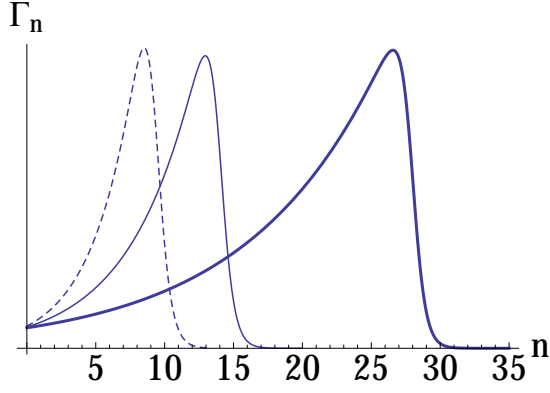


FIG. 6. Decay rate coming from n th order rearrangements in system and bath, Γ_n , in the presence of a self-consistent Lorentzian bath, as $\Xi \log K - 1$ is tuned towards zero [specifically, for $\Xi \log K - 1 = 0.55$ (dashed), 0.3 (thin) and 0.15 (bold)]. The vertical axes of the three plots are rescaled for clarity. The self-consistent bath linewidth scales as in Eq. (19).

$$\left(\frac{\Gamma_2^2}{\Gamma_1 \delta_m} \right)^{\min(1, \frac{1}{\Xi \log K})} \ll \frac{\Gamma_2^2}{\Gamma_1 \gamma} \ll 1 \quad (22)$$

These conditions are trivially satisfied in the regime of $\Xi \log K \lesssim 1$. In the other case, for $\gamma \ll \delta_m$, the first condition is always satisfied near $\Xi \log K \approx 1$, justifying the Golden Rule. The second condition always holds near $\Xi \log K \approx 1$ so long as

$$\frac{\gamma}{\delta_m} \ll \frac{1}{(zN^2)\Xi \log K}, \quad (23)$$

and is therefore satisfied for $\gamma/\delta_m \ll 1/(zN^2)$. For a given value of γ , therefore, Eq. 22 fails if N is too large or the system is too far from the transition.

We also note that our calculation carved up the system into correlation volumes of fixed length L . However, the linewidth Γ also defines a length scale, and when Γ becomes small enough that this self generated length scale exceeds L then this indicates that our basic setup is no longer appropriate. Equivalently, when the apparent line broadening becomes smaller than the many body level spacing on the dot $\Gamma_2^2/\Gamma_1 < \Delta \exp(-N)$, then evidently the correlations between dots become crucial, and our approach is no longer reliable.

We now estimate when this condition is violated. As relaxation is slowest for $\Xi \log K \ll 1$, we shall address this regime, where, to leading order, the requirement for validity of our approach is that

$$N \gg \left(\frac{\delta_m}{\gamma N^2} \right)^{1/d} \exp \left(\frac{2}{\Xi d} (1 - \Xi \log K) \right) \quad (24)$$

From the construction of the coupled-dot model, we observe that N is approximately L^d , where L is the correlation length; thus, Eq. (24) can be interpreted as a relation between real-space correlation length and Fock-space localization length that must be satisfied in order for our approach to make sense. For small enough Ξ (i.e., for weak enough intra-dot interactions) the condition is surely violated, so that a mean-field description is no longer justifiable. We conjecture that, at least in $d \gg 1$, the localization transition occurs in this regime. We note also that the range of validity of our theory can be extended to arbitrarily small (but non-zero) Γ by making N appropriately large and scaling γ accordingly, i.e., we can describe a ‘bad metal’ that is arbitrarily close to localization, although we cannot describe the localization transition itself.

Finally, we note that even when our mean-field approach yields a metallic phase as the only stable solution, it does not directly imply the instability of the insulator in an isolated system. One reason for this is our assumption that the (presumptively thermalizing) bath is much larger than the system. This assumption is valid if one is considering a system that is weakly coupled at its boundaries to a thermodynamically large bath (see Appendix B), or exploring the stability of the nearly localized metal to the nucleation of insulating regions inside it. It is not clear, however, how such a large thermalizing region would nucleate starting from the MBL phase. We cannot rule out the interesting possibility that an MBL system weakly coupled to a bath at its boundaries might exhibit qualitatively different behavior, even deep in the bulk, from a perfectly isolated MBL system.

V. CONCLUSIONS

We have argued that a many-body localized system coupled to a slowly fluctuating external bath exhibits rich relaxational dynamics due to collective hops; in particular, the relaxation time diverges as a power law of the bandwidth of the bath. We have argued that our results apply to a wide range of realistic experiments. The slow relaxational dynamics due to an extrinsic (e.g., nuclear-spin) bath is intimately related to the slowing of relaxation as the MBL transition is approached; thus, as we have discussed, the narrow-band relaxation results can be used to construct a self consistent mean-field description of a metal near the MBL transition (i.e., in the regime where the intrinsic relaxation timescales are parametrically slower than the characteristic dynamical timescales of the system). The key quantity that we examine as a diagnostic of proximity to the localized phase is the typical width of a local spectral line; this quantity, which is related to observables such as the DC conductivity, would be strictly zero in the localized phase. While we are able to determine how this typical spectral linewidth scales to zero as a function of various parameters, we find that the linewidth (and hence the DC conductivity) is nonzero

everywhere within the range of validity of our mean field theory, such that we cannot actually access the phase transition (as is the case with almost all mean field theories). However, we can describe the metallic phase arbitrarily close to localization. This metallic phase should exhibit much of the phenomenology discussed in Ref.¹⁷, including the existence of gaps at multiple scales in the local spectral functions, and of a (weakly filled-in) soft gap at $\omega = 0$ in the spatially averaged spectral functions of local operators. Our mean-field approach, which consists of treating a correlation volume as a zero-dimensional, in-

teracting system coupled to a self-consistent bath, should be generalizable to a wide range of models with MBL transitions.

Acknowledgments. We are indebted to David Huse, Ariel Amir, Michael Knap, Norman Yao, Eugene Demler, and Mikhail Lukin for helpful discussions; and to David Huse and Ariel Amir for a critical reading of this manuscript. This research was supported in part by the Harvard Quantum Optics Center (SG) and by a PCTS fellowship (RN), and began at the Boulder summer school for condensed matter physics.

-
- ¹ P. W. Anderson, Phys. Rev. **109**, 1492 (1958).
 - ² L. Fleishman and P. W. Anderson, Phys. Rev. B **21**, 2366 (1980).
 - ³ I. V. Gornyi, A. D. Mirlin, and D. G. Polyakov, Phys. Rev. Lett. **95**, 206603 (2005).
 - ⁴ D. Basko, I. Aleiner, and B. Altshuler, Ann. Phys. **321**, 1126 (2006).
 - ⁵ V. Oganesyan and D. A. Huse, Phys. Rev. B **75**, 155111 (2007).
 - ⁶ M. Znidaric, T. Prosen, and P. Prelovsek, Phys. Rev. B **77**, 064426 (2008).
 - ⁷ A. Pal and D. A. Huse, Phys. Rev. B **82**, 174411 (2010).
 - ⁸ D. A. Huse, R. Nandkishore, V. Oganesyan, A. Pal, and S. L. Sondhi, Phys. Rev. B **88**, 014206 (2013).
 - ⁹ D. Pekker, G. Refael, E. Altman, and E. Demler, arXiv:1307.3253 (2013).
 - ¹⁰ R. Vosk and E. Altman, arXiv:1307.3256.
 - ¹¹ R. Vosk and E. Altman, Phys. Rev. Lett. **110**, 067204 (2013).
 - ¹² M. Serbyn, Z. Papić, and D. A. Abanin, Phys. Rev. Lett. **110**, 260601 (2013); Phys. Rev. Lett. **111**, 127201 (2013).
 - ¹³ D. A. Huse and V. Oganesyan, arXiv:1305.4915 (2013).
 - ¹⁴ B. Bauer and C. Nayak, arXiv:1306.5753 (2013).
 - ¹⁵ D. A. Huse, R. Nandkishore, and V. Oganesyan, in preparation (2014).
 - ¹⁶ J. A. Kjäll, J. H. Bardarson, and F. Pollmann, arXiv:1403.1568 (2014).
 - ¹⁷ R. Nandkishore, S. Gopalakrishnan, and D. A. Huse, arXiv:1402.5971.
 - ¹⁸ L. S. Levitov, Phys. Rev. Lett. **64**, 547 (1990).
 - ¹⁹ A. L. Burin, Y. Kagan, L. A. Maksimov, and I. Y. Polishchuk, Phys. Rev. Lett. **80**, 2945 (1998).
 - ²⁰ N. Y. Yao, C. R. Laumann, S. Gopalakrishnan, M. Knap, M. Mueller, E. A. Demler, and M. D. Lukin, ArXiv e-prints (2013), arXiv:1311.7151 [cond-mat.stat-mech].
 - ²¹ B. L. Altshuler, Y. Gefen, A. Kamenev, and L. S. Levitov, Phys. Rev. Lett. **78**, 2803 (1997).
 - ²² C. Laumann, A. Pal, and A. Scardicchio, arXiv:1404.2276 (2014).
 - ²³ We note that there are some similarities between Section IV and Ref.42. However, 42 is concerned with the localization transition for single excitations above the ground state, whereas we are concerned with the very different problem of the localization transition for generic high energy states. Moreover, unlike 42 we work on a regular lattice (not a Bethe lattice), and incorporate Hartree terms; as we discuss, this changes the nature of metallic-state solutions.
 - ²⁴ N. F. Mott, J. Non-Crystalline Solids **1**, 1 (1968).
 - ²⁵ M. Serbyn *et al.*, arXiv:1403.0693.
 - ²⁶ A. V. Khaetskii, D. Loss, and L. Glazman, Phys. Rev. Lett. **88**, 186802 (2002).
 - ²⁷ A. Khaetskii, D. Loss, and L. Glazman, Phys. Rev. B **67**, 195329 (2003).
 - ²⁸ W. M. Witzel and S. Das Sarma, Phys. Rev. B **74**, 035322 (2006); L. Cywiński, W. M. Witzel, and S. Das Sarma, Phys. Rev. Lett. **102**, 057601 (2009).
 - ²⁹ N. Bloembergen, Physica **15**, 386 (1949); A. Szabo, T. Muramoto, and R. Kaarli, Phys. Rev. B **42**, 7769 (1990).
 - ³⁰ P. Cappellaro, L. Jiang, J. S. Hodges, and M. D. Lukin, Phys. Rev. Lett. **102**, 210502 (2009).
 - ³¹ A. Amir, J. J. Krich, V. Vitelli, Y. Oreg, and Y. Imry, Phys. Rev. X **3**, 021017 (2013).
 - ³² A. Georges, G. Kotliar, W. Krauth, and M. J. Rozenberg, Rev. Mod. Phys. **68**, 13 (1996).
 - ³³ V. Dobrosavljevic, A. A. Pastor, and B. Nikolic, Europhys. Lett. **62**, 76 (2003); M. C. O. Aguiar, V. Dobrosavljević, E. Abrahams, and G. Kotliar, Phys. Rev. Lett. **102**, 156402 (2009).
 - ³⁴ A. Amir, Y. Lahini, and H. B. Perets, Phys. Rev. E **79**, 050105 (2009).
 - ³⁵ A. Amir, in preparation.
 - ³⁶ In a homogeneous system, the MBL transition occurs at $g \lesssim 1$; however, as we are considering a system of coupled grains, we may consistently assume that $g \gg 1$.
 - ³⁷ I. L. Aleiner, P. W. Brouwer, and L. I. Glazman, Phys. Rep. **358**, 309 (2002).
 - ³⁸ Note that, although the *single-particle* properties are described by random-matrix theory, in general the *many-body* level statistics are not.
 - ³⁹ R. Abou-Chacra, P. W. Anderson, and D. J. Thouless, J. Phys. C **6**, 1734 (1973); J. T. Chalker and S. Siak, J. Phys.: Condensed Matter **2**, 2671 (1990).
 - ⁴⁰ X. Leyronas, P. G. Silvestrov, and C. W. J. Beenakker, Phys. Rev. Lett. **84**, 3414 (2000); A. M. F. Rivas, E. R. Mucciolo, and A. Kamenev, Phys. Rev. B **65**, 155309 (2002).
 - ⁴¹ The l-bit model of the FMBL state is unsuitable for our present purposes, because it has a decay length for the interactions which diverges near the localization transition, and we want a model where the interactions are short range.
 - ⁴² M. V. Feigel'man, L. B. Ioffe, and M. Mézard, Phys. Rev. B **82**, 184534 (2010).

⁴³ We can justify using *typical* frequencies for the centers of the bath lines because, upon the removal of rare resonances, the spectrum of the two-particle hopping operator contains a soft gap¹⁷. Thus, the bath spectrum contains a soft gap at the location of each system transition, and this soft gap is “filled in” with weight $\propto \Gamma_2$ by the tails of Lorentzians. Our theory is not meant to describe the (presumably metallic) regime in which nearest-neighbor resonances have proliferated.

⁴⁴ J. Z. Imbrie, arXiv:1403.7837 (2014).

Appendix A: Gaussian and Lorentzian baths

The arguments in the main text were framed in terms of a bath with a constant density of states over a window $[-W/2, W/2]$. We now generalize these results to baths with spectra that are Gaussian (e.g., a nuclear spin-bath) and Lorentzian (e.g., a self-consistent bath). For concreteness, we shall focus on the relaxation rate Eq. (5), but the generalization to the other main results in the main text is straightforward.

Gaussian bath

First, we consider the case of a bath with the density of states $N(E) \sim \exp[-(E/W)^2]/W$. Applying the Golden Rule, we find that the relaxation rate of an n^d -particle rearrangement goes as

$$\Gamma_n \sim \frac{\gamma^2}{W} \exp\left(-\frac{2n^d}{\Xi} - \frac{\Delta^2}{W^2} e^{-2s(T)n^d}\right). \quad (\text{A1})$$

One can optimize Γ_n by steepest-descent methods. The solution is:

$$\hat{n}^d = \frac{1}{2s(T)} \log\left(\frac{\Delta^2}{W^2} \frac{\Xi s(T)}{2}\right) \quad (\text{A2})$$

which agrees, up to logarithmic corrections, with Eq. (5).

Lorentzian bath

As discussed in the main text surrounding Eq. (15), the case of a Lorentzian bath has two distinct regimes, depending on whether the matrix element decreases faster or slower than the density of states increases as we go to higher order in Fock space. One can see this as follows: for a decay process that uses the tails of the Lorentzian (of width W), the Golden-Rule decay rate can schematically be written as $W(\text{matrix element/energy denominator})^2$. The quantity in parentheses is precisely the perturbative expression for the wavefunction amplitude on the target site; therefore, this quantity (and the Golden-Rule decay rate) must decay with n whenever the

wavefunction is localized. To state this more quantitatively: for a density of states $N(E) \sim W/(E^2 + W^2)$, the typical matrix element for an n th order process is suppressed as $e^{-n/\Xi}$. By contrast, the level spacing scales as $\exp(-s(T)n)$. Localization at a given temperature requires that $s(T)\Xi < 1$.

The regime of collective relaxation for a Lorentzian bath only exists (on a Cayley tree) when $\Xi \log K > 1$. Here, the relaxation rate of an n -step hop goes as

$$\Gamma_n \sim \frac{\gamma^2}{W} \frac{e^{-2n/\Xi}}{(\Delta/W)^2 e^{-2n \log K} + 1} \quad (\text{A3})$$

Optimizing with respect to n yields the condition

$$e^{-2n \log K} = \frac{W^2}{\Delta^2} \frac{1/\Xi}{\log K - 1/\Xi}, \quad (\text{A4})$$

which leads to the solution

$$\hat{n} = \frac{1}{\log K} \left[\log(\Delta/W) + \frac{1}{2} \log(\Xi \log K - 1) \right] \quad (\text{A5})$$

which is again the same form as that in the main text.

Finally we comment on the case in which the wings of the Lorentzian have a hard (or Gaussian) cutoff at an energy Λ . In this case, the lowest-order process that the bath can mediate is at the order $n_0 \sim \log(\Delta/\Lambda)/\log K$. When $\Xi \log K < 1$, one can conclude from the arguments above that relaxation takes place at exactly this order, and crucially, that the optimal order in perturbation theory is *independent* of W .

Appendix B: Inhomogeneous mean-field equations

This Appendix discusses the inhomogeneous generalizations of the mean-field equations (12), (15) in the main text. The generalization of Eq. (15) is obvious—one treats each site as a separate self-consistent bath and adds up the decay rates coming from coupling to each site—but that of Eq. (12) is more delicate, as it involves understanding which states contribute to the linewidth of a level. For simplicity, we shall address this question for a one-dimensional system.

We are interested in the broadening of a level on dot I as a result of decay processes on dots J sites away. The relevant scales in this problem are (a) $\Gamma_2(I)$, the linewidth at dot I after including processes nearer than J sites away; (b) $\Gamma_1(I \pm J)$, the decay rate at sites $I \pm J$; and (c) $\mathcal{U}(J) \equiv \gamma \exp(-|I - J|)$, the interdot coupling at this scale. The rules for self-consistently estimating the contributions to the linewidth at site I are then as follows:

(1) When $\mathcal{U}(J) \ll \Gamma_2(I)$, the level at site I cannot resolve fluctuations at site J , so these do not affect the linewidth.

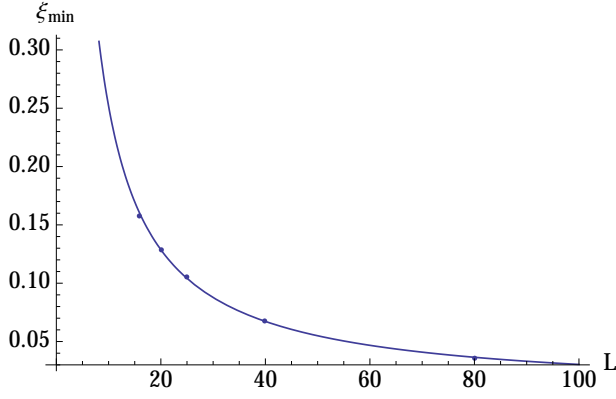


FIG. 7. Dependence on the parameter $\xi_{min} \sim \gamma/\delta$ of the minimum system size required for a self-sustaining bulk metallic solution, in the case where $\Gamma_{1,2}$ are pinned to zero at both boundaries. We find that $\xi_{min} \sim 1/L$; thus, as $L \rightarrow \infty$, $\xi_{min} \rightarrow 0$ as expected from the discussion in the main text.

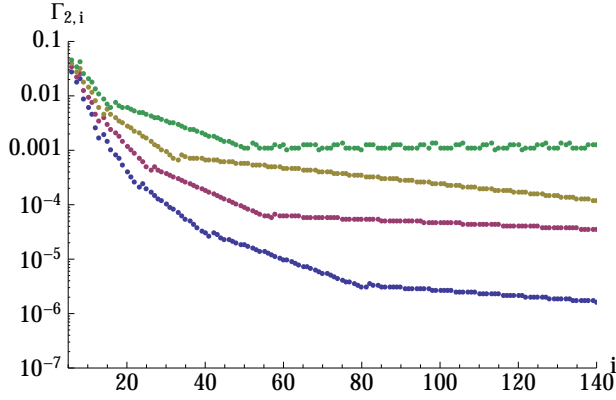


FIG. 8. Falloff of the linewidth in the case where the system is subject to a relatively strong bath at its left boundary: results (on a semilog scale) for relatively small chains ($L = 150$) for $\gamma/\delta_m = 0.12, 0.14, 0.16, 0.18$; the falloff of the linewidth can be described as a sum of exponentials.

(2) When $\mathcal{U}(J) \gg \Gamma_2(I), \Gamma_1(J)$ then each spin-flip on site J (with rate $\Gamma_1(J)$) causes the level I to fluctuate more than a linewidth; the associated contribution to the linewidth at site I is $\Gamma_1(J)$.

(3) When $\Gamma_1(J) \gg \mathcal{U}(J) \gg \Gamma_2(I)$, then spin J flips many times in the interval $1/\mathcal{U}(J)$, and its effects on spin I mostly average out. In this regime, which is reminiscent

of “motional narrowing”³⁴, the contribution to $\Gamma_2(I)$ is given by $\mathcal{U}(J)^2/\Gamma_1(J)$.

These rules can be combined into a mean-field equation of the form $\Gamma_2(i) = \sum_j f(|j - i|; \Gamma_1(j))$, where f has the asymptotic behavior discussed above. Figs. 7, 8 describe properties of the numerical solutions with two kinds of boundary conditions. First, we consider the case in which one pins $\Gamma_{1,2} = 0$ at both boundaries (but seed the system with a small decay rate in the interior).

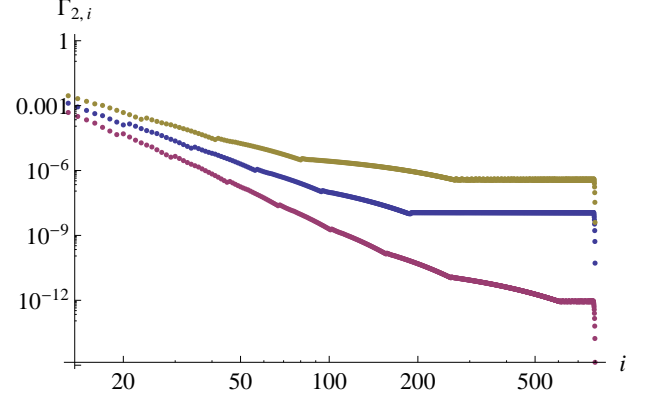


FIG. 9. Numerical solution for $\gamma/\delta_m = 0.08, 0.1, 0.12$ on much larger system sizes ($L = 800$) on a log-log scale. Notice that the falloff of the linewidth is essentially power law over many decades of Γ_2 and at least one decade of L .

For simplicity we have not included the disorder in the localization length—this can be justified in the small-decay limit as each degree of freedom averages over a large spatial range. We find that, when γ/δ_m is above a size-dependent critical value, the bulk reaches a constant value of $\Gamma_{1,2}$; by contrast, when γ/δ_m is less than its critical value, the stable solution has $\Gamma_{1,2} = 0$. The size-dependence of this critical value is plotted in Fig. 7; one can see that it fits well to the form $(\gamma/\delta) \sim 1/L$, which asymptotes to zero in the thermodynamic limit (consistent with the fact that we find no stable uniform localized state). Second, we consider the case in which the edges are connected to a bath with a relatively large decay rate; in this case, the linewidth saturates increasingly slowly to its steady-state value (Figs. 8, 9). For small localization lengths, the decay to the steady-state linewidth is power-law to a good approximation. Intuitively, one can understand this slow decay as a consequence of the fact that as one moves farther from the edge and the self-consistent linewidth decreases, each level becomes sensitive to increasingly many neighbors.